DE GRUYTER Journal of the Mechanical Behavior of Materials 2024; 33: 20240007

Research Article

Martin Wijaya, Aswin Lim*, Paulus Pramono Rahardjo, Alfrendo Satyanaga, Abdul Halim Hamdany and Glenn Adriel Adiguna

Determination of soil–water characteristic curves by using a polymer tensiometer

https://doi.org/10.1515/jmbm-2024-0007
received January 15, 2023; accepted May 24, 2024

Abstract: Recently, rainfall-induced slope failure has struck Cimanggung village, West Java province, Indonesia. In order to anticipate future slope failures due to rainfall, an unsaturated slope stability analysis is compulsory. Precise information on the soil–water characteristic curve (SWCC) is required to conduct an accurate unsaturated soil analysis. In this article, a procedure to obtain SWCC by using a polymer tensiometer for Cimanggung village is proposed. Considering the long period of time needed to obtain the measured data, some prediction methods are available. The measured SWCCs are then compared with SWCCs based on two prediction methods. Chin's 1-point and Perera *et al.*'s methods are applied as the prediction methods and then compared with the measured SWCCs. It could be concluded that Chin's 1-point method yields a close estimation within the suction range. Meanwhile, the Perera *et al.* method underestimates the air entry value, and the predicted curve deviates significantly with the measured SWCC. Hence, Chin's 1-point method is recommended for predicting SWCCs in Cimanggung Village.

Keywords: polymer tensiometer, unsaturated soil, suction measurement, SWCC, Cimanggung

*** Corresponding author: Aswin Lim,** Civil Engineering Department, Faculty of Engineering, Universitas Katolik Parahyangan, Jl. Ciumbuleuit No. 94, Hegarmanah, Kec. Cidadap, Kota Bandung, Jawa Barat, 40141, Indonesia, e-mail: aswinlim@unpar.ac.id
Martin Wijaya, Paulus Pramono Rahardjo, Glenn Adriel Adiguna: Civil Engineering Department, Faculty of Engineering, Universitas Katolik Parahyangan, Jl. Ciumbuleuit No. 94, Hegarmanah, Kec. Cidadap, Kota Bandung, Jawa Barat, 40141, Indonesia
Alfrendo Satyanaga: Department of Civil and Environmental Engineering, Nazarbayev University, 53, Kabanbay Batyr Ave, 010000, Nur-Sultan, Kazakhstan
Abdul Halim Hamdany: Department of Civil Engineering, Faculty of Engineering, Universitas Indonesia, Depok, Jawa Barat, 16424, Indonesia

1 Introduction

The role of the soil–water characteristic curve (SWCC) is not limited to serving as an input parameter for the transient flow analysis in unsaturated soil [1] but is also one of the most reliable parameters to estimate the shear strength [2–8] and permeability [9–13] of unsaturated soil which are a function of soil suction. Zhai *et al.* [14] used a contact angle method to estimate SWCC from the grain-size distribution of coarse-grained soil. Zhai *et al.* [15,16] used both "ink-bottle" and "rain-drop" effects to estimate the hysteresis of SWCC and unsaturated permeability of soil. The hysteresis path of SWCC and unsaturated permeability of soil resulting from wetting–drying cycles is important to conduct slope stability analysis [17].

There are three types of SWCCs [18], which are the gravimetric-based SWCC (SWCC-w), the volumetric-based SWCC (SWCC-θ), and the degree of saturation-based SWCC (SWCC-S). SWCC-w is the easiest to obtain as it is not required to measure the volume change of unsaturated soil specimens due to the change in soil suction [19–21]. The effect of density and stress dependency on SWCC-w has also been investigated by several researchers [22–26]. The investigations have shown that the effect of density (either due to compaction or consolidation) on coarse-grained and fine-grained soils only affects the initial part of the curve and will merge into the virgin drying line, as illustrated in Figure 1. However, it is important to note that the input for the flow analysis in unsaturated soil requires SWCC-θ, while the determination of the unsaturated permeability function and air entry value (AEV) requires SWCC-S [11,12,18]. Hence, it is imperative to obtain all the three SWCCs. For coarse-grained soil, there will be no change in volume due to the change in soil suction. Hence, SWCC-w, SWCC-θ, and SWCC-S will provide similar information [18]. However, there will be a significant change in soil volume due to the change in soil suction when it comes to fine-grained soil. Suction on fine-grained soil can be extremely high, especially when there is a vegetation on the sloping ground. The significant increase in soil suction may affect

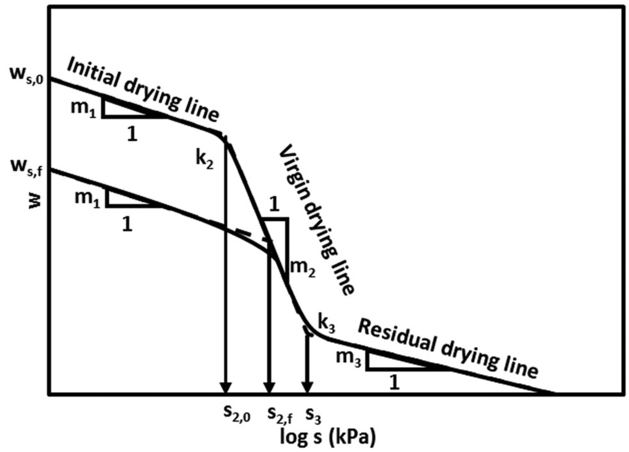

Figure 1: Effect of density on SWCC-*w* [24].

the hydraulic properties of unsaturated soil [27]. Hence, conversion between SWCCs will be very important. As it is difficult to measure the volume change during the SWCC test, it is recommended to construct a shrinkage curve (a curve that represents a change in the void ratio due to the change in the gravimetric water content) to convert SWCC-*w* to SWCC-*θ* and SWCC-*S* [18,28,29].

On 9 January 2021, heavy rainfall (143 mm/day) induced slope failure at Cimanggung (Figure 2) and caused significant death toll and destruction of properties in the landslide vicinity [30]. Due to the landslide, most of the people living in the landslide vicinity were temporarily evacuated and arose a necessity to take a decision on whether the housing in the landslide area could be reconstructed after the landslide. Rainfall-induced slope failure has been assessed in the Cimanggung slope using estimated unsaturated soil properties [31]. In order to make a proper assessment of the potential of a future landslide due to the rainfall that might occur, it is important to obtain an SWCC, which is one of the main soil properties in unsaturated soil analysis [18]. In this article, an SWCC for volcanic soil in Indonesia is proposed which can be applied as a volcanic soil SWCC database for other regions in the world. SWCC can be obtained from direct measurement of suction using a tensiometer. However, conventional tensiometers generally only be able to measure suction up to 90 kPa. In this article, the focus is on developing a procedure to determine SWCC-*w* from the debris of the slope and how it is compared with a typical prediction method which is used as no data are available. The objective of this article is to establish a procedure to obtain SWCC-*w*, SWCC-*θ*, and SWCC-*S* in the most economical way by using a polymer tensiometer developed by Umwelt-Geräte-Technik (UGT) that can measure the matric suction up to 1,500 kPa, and there is no requirement for maintenance (flushing due to diffusion), so that it is possible to do a long-term measurement. Comparison will also be carried out to evaluate the suitability of some prediction methods for soil at Cimanggung village.

Figure 2: Aerial photo of Cimanggung slope failure.

2 Background theory

SWCC-θ could be determined once a shrinkage curve is obtained as follows:

$$\theta(s) = \frac{w \cdot G_s}{1 + e}, \quad (1)$$

where $\theta(s)$ is the volumetric water content as a function of soil suction and w is the gravimetric water content that can be obtained from SWCC-w and is a function of soil suction and void ratio (e). Those parameters could be obtained from the shrinkage curve. Similarly, SWCC-S can also be obtained through the following relationship:

$$S_r(s) = \frac{w \cdot G_s}{e}. \quad (2)$$

SWCC can be constructed by either reducing the water content of the soil and then measuring its suction or by controlling the soil suction and then measuring the water content. Suction measurement can be done either by using a direct measurement method where the pore water pressure (u_w) is directly measured to determine the soil suction or an indirect measurement method in which other properties are used to determine soil suction [32]. Regardless of the methods that are used to construct the SWCC, the range of suction that can be measured is limited by the apparatus. For instance, a tensiometer (direct measurement) is unable to measure the pore pressure less than −101 kPa due to the cavitation phenomenon [33–35]. A way to overcome the limitation of direct measurement is either by using an axis translation apparatus [34,36] or by employing a high-capacity tensiometer (HCT) [32,33,37–42].

In the axis translation apparatus, the air pressure (u_a) is increased such that the pore water pressure (u_w) is also increased to avoid cavitation [34,36]. The maximum air pressure that can be applied depends on the amount of air that enters the high-air entry (HAE) disk, with the maximum value typically around 1,500 kPa. The equilibrium time required to measure the soil suction may range from a few hours to days depending on the type of soil. An HCT is developed to directly measure soil suction as high as 1,500 kPa. The reason behind HCT can extend the range of suction measurement beyond 101 kPa is that due to the use of demineralized water, the water in the small water compartment between the transducer and the HAE disk is pressurized under very high pressure to remove all the air bubbles in the water compartment [37,38]. The problem with HCT is that once it is used for a long period of time, it may cavitate despite not reaching its maximum capacity, and once it is cavitated, the HCT needs to be repressurized [41].

In the indirect measurement method, the soil suction is measured by using other properties such as filter paper [43,44] or chilled mirror hygrometer [45]. The indirect measurement typically has a much wider range of suction measurements but unsuitable for the low suction range [46]. Looking at the limitations that come from different apparatuses, it is difficult to obtain the entire range of SWCCs [47]. While it is possible to use different apparatuses to obtain the entire range of SWCCs, the cost of purchasing different apparatuses to measure soil suction makes it practically difficult for industrial laboratories to use it as a routine practice. Another problem is the test duration to obtain sufficient data to construct SWCCs.

The most recent development in suction measurement is using a polymer-based or an osmotic tensiometer [47–53]. In a polymer-based tensiometer, a polymer solution is placed inside a membrane that is permeable to the soil solution but impermeable to the polymer solution [50]. The polymer tensiometer is pre-saturated so that the polymer solution absorbs the water and generates a swelling pressure, sometimes referred to as the osmotic pressure [47]. The maximum osmotic pressure which is obtained through pre-saturation is referred to as P_{ref}. When the polymer tensiometer is in contact with unsaturated soil, there will be a pressure drop inside the polymer tensiometer ($P_{current}$). The drop in pressure is assumed to be equal to the increase in uncorrected soil suction (s_{uncor}), and hence soil suction can be calculated as follows [47,50]:

$$s_{uncor} = p_{ref} - p_{current}. \quad (3)$$

The first polymer tensiometer was perhaps developed by Peck and Rabbidge [51]. The conventional tensiometer generally can only measure suction up to 90 kPa. The polymer tensiometer is attractive due to its potential to measure high suction, with the maximum suction measured to be about 1,000–1,500 kPa; it can be pre-saturated using a simple water bath without any water pressure to reach its full capacity, has no issue with cavitation, and hence can be easily adopted for *in situ* measurement [47–50,53]. However, several issues related to polymer tensiometer have been addressed by Bocking and Fredlund [54], such as the polymer tensiometer suffering gradual loss of pressure (pressure decay), unknown zero drift, temperature effects, and slow equilibration times, which then halted the development of polymer tensiometer at that time [50].

Figure 3a shows the decay in osmotic pressure measured by van der Ploeg [50], while Figure 3b shows the effect of temperature on the osmotic pressure. Figure 4 shows the decay in suction and the effect of temperature on the suction measurement using a polymer tensiometer

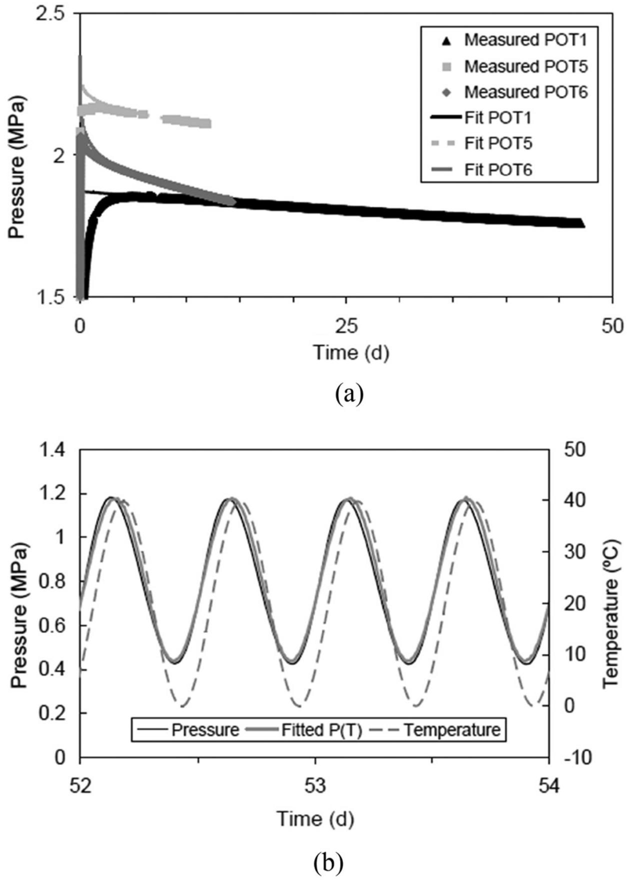

Figure 3: (a) Pressure decay and (b) temperature effect [50].

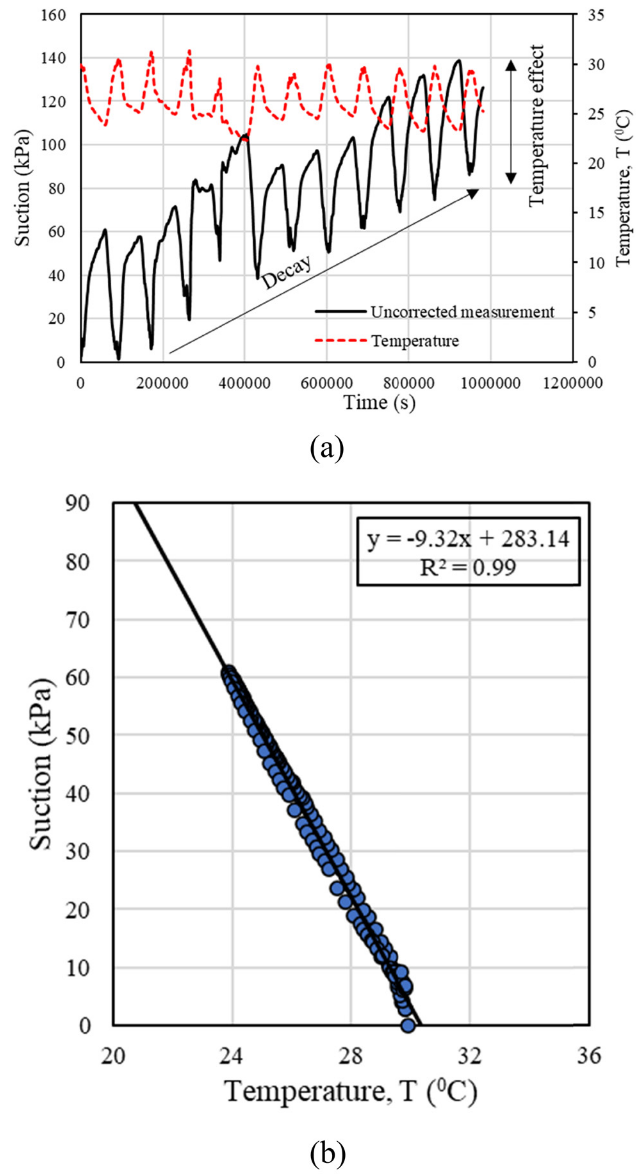

Figure 4: (a) Effect of pressure decay and temperature effect on suction measurement and (b) temperature correction [47].

conducted by Hamdany *et al.* [47]. Pressure decay is suspected due to polymer degradation or by diffusion of some smaller-sized polymer molecules through the membrane [47,50] and hence requires a correction to be applied. van der Ploeg [50] observed that the pressure decay gradually became less (or exponential decay) and proposed the following correction for pressure decay:

$$\pi_t = b \exp - (t/\tau)^c, \tag{4}$$

where π_t is the pressure decay correction, t is the time, and b, τ, and c are curve-fitting parameters. On the other hand, Peck and Rabbidge [52] and Hamdany *et al.* [47] observed a linear decay. Hamdany *et al.* [47] proposed a linear correction as follows:

$$\pi_t = m_\mathrm{d}(t - t_0), \tag{5}$$

where m_d is the curve-fitting parameter and t_0 is the time when the probe is fully saturated. For temperature correction, van der Ploeg [50] proposed a quadratic function as follows:

$$\frac{P_T - P_0}{P_0} = C_1\left(\frac{T - T_0}{T_0}\right)^2 + C_2\left(\frac{T - T_0}{T_0}\right) + C_3, \tag{6}$$

where P_t is the pressure at temperature T, P_0 is the reference pressure at reference temperature T_0, and C_1, C_2, and C_3 are curve-fitting parameters. An example of the fitted equation is shown in Figure 3b. Hamdany *et al.* [47] proposed employing linear regression to fit the change in suction (Ds_t) with temperature, as shown in Figure 4b. Soil suction (uncorrected with pressure decay) can then be calculated as follows:

$$s_t = s_\mathrm{uncor} - \Delta s_T. \tag{7}$$

The corrected soil suction (s) can then be corrected as follows [47]:

$$s = s_t - \Delta s_\mathrm{d}. \tag{8}$$

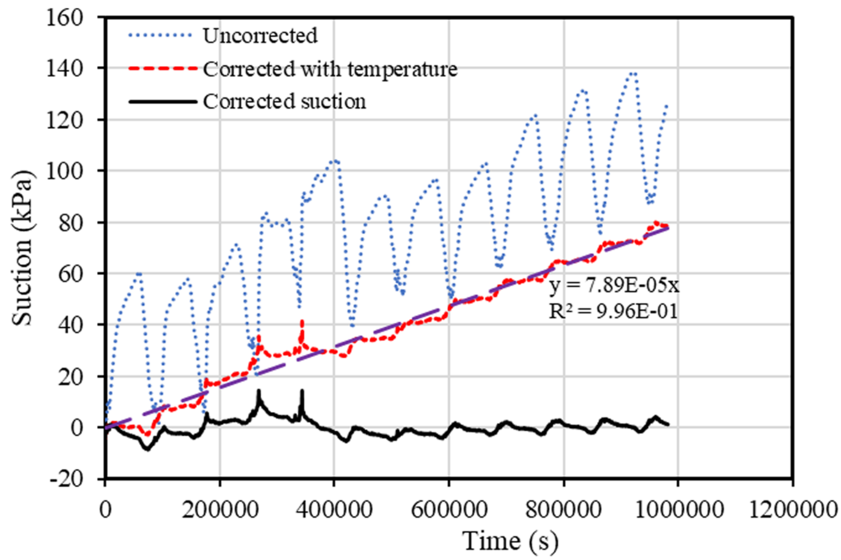

Figure 5: Correction for temperature and pressure [47].

Figure 5 shows the correction for temperature and pressure conducted by Hamdany *et al.* [47]. Extensive research has been carried out by Degré *et al.* [48] to compare the SWCC obtained from the polymer tensiometer and the matric potential sensor (MPS) with a reference SWCC (constructed by using five intact soil cores), and by van der Ploeg *et al.* [53] where a sand box (0–9.8 kPa suction), suction plates (9.8–59 kPa suction), and a pressure plate (100–1,500 kPa suction) are used to construct the SWCC (Figure 6). It is shown that the polymer tensiometer appears to agree very well with the reference curve, which shows the capability of the polymer tensiometer. It is interesting to note that there appears to be no decay in the polymer tensiometer used by Degré *et al.* and van der Ploeg *et al.* [48].

UGT developed a polymer tensiometer (Figure 7), which is referred to as a full-range tensiometer (FRT). The polymer-based tensiometer is typically affected with the decay issue, as described in the literature review. However, the UGT polymer tensiometer is unaffected by decay. The capacity of the UGT polymer tensiometer is around 2,000 kPa. The UGT polymer tensiometer is claimed to be maintenance-free and can remain in the field for a very long period due to low power consumption. The UGT polymer tensiometer measurement is also reliable in difficult media such as in saline sites. The temperature correction to the P_{ref} is given by:

$$p_{\mathrm{ref}} = C_{T1} \cdot T_{\mathrm{current}}^{2} + C_{T2} \cdot T_{\mathrm{current}} + P_0, \tag{9}$$

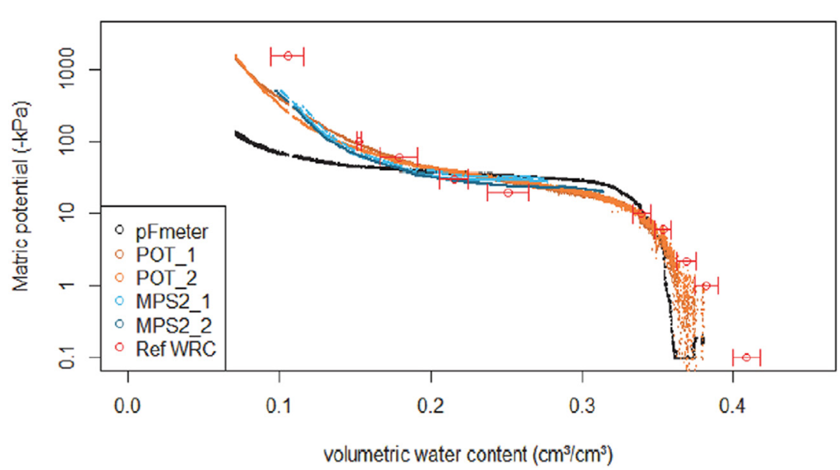

Figure 6: Comparison between MPS and the polymer tensiometer (POT) with a reference water retention curve from van der Ploeg *et al.* [53] conducted by (Degré *et al.* [48].

Figure 7: Components of FRT.

where C_{T1} and C_{T2} are curve-fitting parameters, P_0 is the reference pressure at 0°C, and $T_{current}$ is the current temperature. Decay correction is only required when there is an offset in the P_0. While the UGT polymer tensiometer is actually meant for *in situ* measurement, it is of interest to use the UGT polymer tensiometer to obtain SWCC in the lab which makes the tensiometer attractive as it can be used in the lab and on the site.

As obtaining SWCCs takes a very long time to finish, the use of an estimation method is sometimes preferred to obtain the SWCC, especially for the case where a quick decision has to be made. Perera *et al.* [55] proposed the use of Fredlund and Xing' [56] degree of saturation-based SWCC (SWCC-*S*), which is expressed as follows:

$$S_r(s) = \frac{C(s)}{\left\{\ln\left[\exp(1) + \left(\frac{s}{a_f}\right)^{n_f}\right]\right\}^{m_f}}$$
$$C(s) = 1 - \frac{\ln\left(1 + \frac{s}{\psi_r}\right)}{\ln\left(1 + \frac{10^6}{\psi_r}\right)}. \quad (10)$$

Determination of a_f, n_f, m_f, and ψ_r depends on the plasticity index (PI) and percent passing sieve No. 200 (P_{200}). Soil is considered as non-plastic granular soil if PI.P_{200}/100 < 1, while it is considered as plastic soil when PI.P_{200}/100 > 1. For non-plastic granular soil, Fredlund and Xing's [56] empirical parameters are given as follows:

$$a_f = \max(1.14a - 0.5, 1)$$
$$a = -2.79 - 14.1\log(D_{20}) - 1.9 \times 10^{-6}P_{200}^{4.34} + 7\log(D_{30}) + 0.055D_{100}, \quad (11a)$$

$$D_{100} = 10^{\left[\frac{40}{m_{1p}} + \log(D_{60})\right]}, \quad (11b)$$

$$m_{1p} = \frac{30}{[\log(D_{90}) - \log(D_{60})]}, \quad (11c)$$

$$n_f = 0.936b - 3.8, \quad (11d)$$

$$b = \left\{5.39 - 0.29\ln\left[P_{200}\left(\frac{D_{90}}{D_{10}}\right)\right] + 3D_0^{0.57} + 0.021P_{200}^{1.19}\right\}m_1^{0.1}, \quad (11e)$$

$$D_0 = 10^{\left[\frac{-30}{m_{2p}} + \log(D_{30})\right]}, \quad (11f)$$

$$m_{2p} = \frac{20}{[\log(D_{30}) - \log(D_{10})]}, \quad (11g)$$

$$m_f = 0.26\exp(0.758c) + 1.4D_{10}, \quad (11h)$$

$$c = \log(m_{2p}^{1.15}) - \left(1 - \frac{1}{n_f}\right), \quad (11i)$$

$$\psi_r = 100, \quad (11j)$$

where D_x is the particle size at percent passing x. For plastic soil, Fredlund and Xing's [56] empirical parameters are given as follows:

$$a_f = 32.853\left\{\ln\left(\frac{P_{200}}{100}\text{PI}\right)\right\} + 32.438, \quad (11k)$$

$$n_f = 1.421\left(\frac{P_{200}}{100}\text{PI}\right)^{-0.3185}, \quad (11l)$$

$$m_f = -0.2154\left\{\ln\left(\frac{P_{200}}{100}\text{PI}\right)\right\} + 0.7145, \quad (11m)$$

$$\psi_r = 500. \quad (11n)$$

Another method is to use Chin's 1-point method [57]. According to Chin's 1-point method, one pair of suction and volumetric water content data is required. The advantage of this method is that as measuring a single suction and water content can be done relatively quick (either in the laboratory or at the site), prediction can be done reasonably fast with a higher degree of confidence (1 data definitely correct). The Chin 1-point method adopted Fredlund and Xing's [56] volumetric water content-based SWCC (SWCC-θ), where the empirical parameters in Fredlund and Xing [56] are correlated with a single empirical parameter χ. In Chin's 1-point method, the soil is classified either as fine-grained soil (P_{200} > 30%) or as coarse-grained soil (P_{200} < 30%). For fine-grained soil, Fredlund and Xing's [56] empirical parameters are given as follows:

$$a_f = -2.4\chi + 722, \quad (12a)$$

$$n_f = 0.07\chi^{0.4}, \quad (12b)$$

$$m_f = 0.015\chi^{0.7}, \quad (12c)$$

$$\psi_r = 914\exp[-0.002(\chi)]. \quad (12d)$$

While for coarse-grained soil, Fredlund and Xing's [56] empirical parameters are given as follows:

$$a_f = 0.53(D_{50})^{-0.96}, \quad (12e)$$

$$n_f = \chi, \quad (12f)$$

$$m_f = -0.23\ln(\chi) + 1.13, \quad (12g)$$

$$\psi_r = 100. \quad (12h)$$

Chin *et al.* [57] recommended that the parameter χ is determined by using soil suction between 300 and 500 kPa. However, predictive methods rely on the soil data which are used as a database. Hence, evaluating predictive methods with actual measurement is important to increase confidence in using a predictive method in practice.

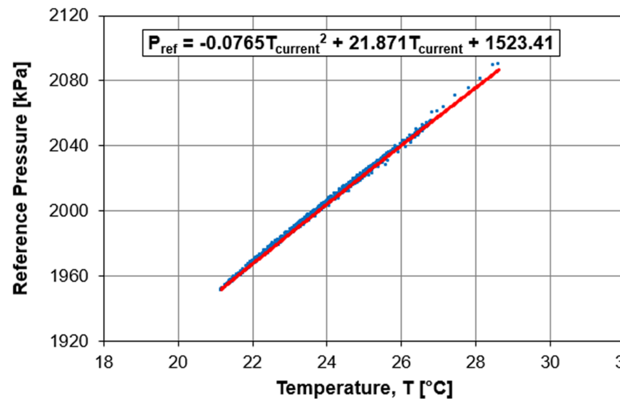

Figure 9: Calibration of FRT.

3 Materials and methods

The procedure to obtain SWCC-*w*, SWCC-*θ*, and SWCC-*S* by using the UGT polymer tensiometer follows the flow chart shown in Figure 8. As it is difficult to obtain undisturbed soil samples of sufficient size, it is recommended to obtain disturbed soil samples which are then reconstituted to obtain SWCC-*w* by using the polymer tensiometer. Undisturbed soil samples are important to characterize the soil state at the site, which could be applied to correct the SWCC-*w* in the field condition and to estimate the shrinkage curve.

Pre-saturation and calibration of the UGT polymer tensiometer are conducted by submerging the tensiometer in a water chamber until the pressure reading reaches its maximum value. Natural fluctuation of temperature and pressure is recorded as shown in Figure 9. No apparent decay is observed during the calibration process. In this research, the quadratic function as described in Eq. (9) is used to calibrate the polymer tensiometer with temperature. C_{T1}, C_{T2}, and P_0 values obtained from the calibration result are −0.0765, 21.871, and 1523.41, respectively.

Soil samples are obtained from the landslide area at Cimanggung village, West Jaya Province, Indonesia (Figure 10). The undisturbed soil sample is obtained from the site to determine the natural state of soil properties. The soil properties are shown in Table 1.

Due to the size of the UGT polymer tensiometer, a larger sample diameter is required. Another batch of disturbed soil samples is obtained in order to be reconstituted

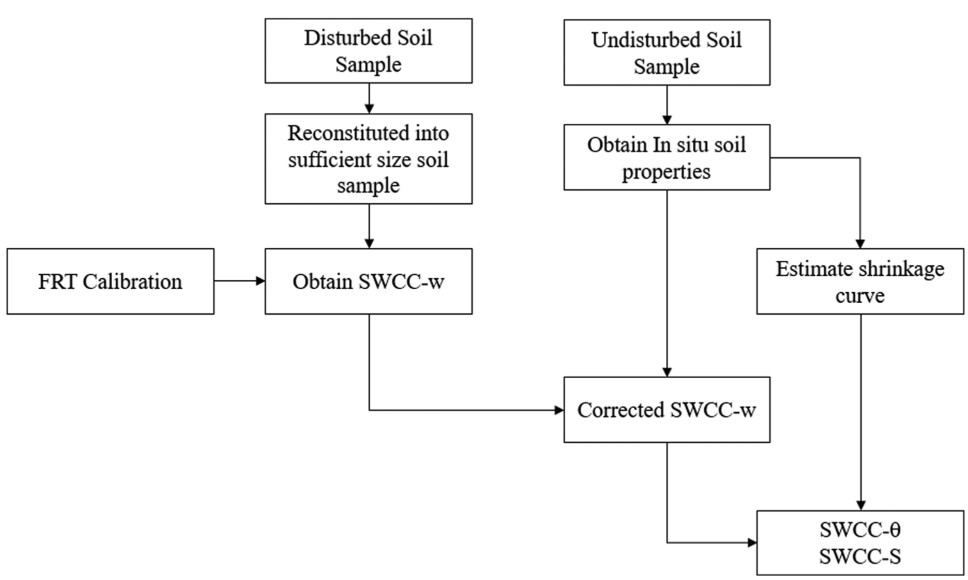

Figure 8: Proposed procedure to obtain SWCC-*θ* and SWCC-*S*.

Figure 10: Soil materials located at the landslide area.

Table 1: Basic soil properties

Soil properties	Values
Specific gravity, G_s	2.53
Liquid limit, LL	54
Plastic limit, PL	31
Index plasticity, IP	23
Bulk density, γ_b (kN/m^3)	17.7
Dry density, γ_d (kN/m^3)	12.6
Natural water content, w_n (%)	36.47
Void ratio, e	1.0
Porosity, n	0.5
Grain size distribution (USCS)	
Sand (%)	15.83
Silt (%)	43.6
Clay (%)	40.6

and then compacted. The initial water content of the compacted soil is about 32.3%. An SWCC is then constructed by air-drying the soil specimen, and the soil suction is measured using the polymer tensiometer shown in Figure 11. The weight of soil is also recorded in order to determine the gravimetric water content (w) of the soil. Once the soil suction reaches around 2,000 kPa, the test is deemed completed. The van Genuchten [10] (VG) SWCC equation was used to curve fit the data points from the polymer tensiometer, which is given as follows

$$w(s) = w_r + \frac{(w_s - w_r)}{[1 + a_v s)n_v]^{m_v}}, \tag{13}$$

where w_s is the saturated gravimetric water content; w_r is the residual gravimetric water content; and a_v, n_v, and m_v are VG's curve-fitting parameters.

As it is of interest to obtain SWCC of the soil at *in situ* conditions, it is of interest to correct gravimetric-based

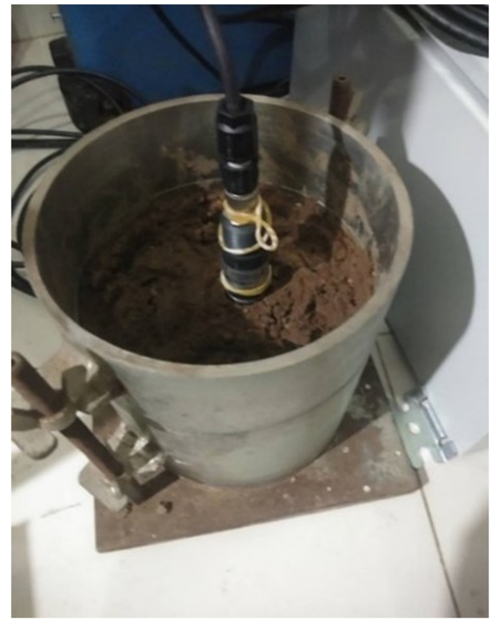

Figure 11: Installation of FRT.

SWCC (SWCC-w) according to the density of the undisturbed soil sample. Correction for SWCC-w under different densities can be done by using Wijaya and Leong [24], which is illustrated in Figure 1 where the effect of density can be reflected by the change in the saturated gravimetric water content ($w_{s,0}$ to $w_{s,f}$) and change in the matric suction at the intersection between the initial drying line and the virgin drying line (from $s_{2,0}$ to $s_{2,f}$). Wijaya and Leong [58] proposed an SWCC equation that uses physically significant parameters and is given as follows:

$$w(s) = w_s - m_1 \log\frac{s}{s_1} - T_2(\log s,\ \log s_1,\ \log s_2, m_2, m_1, k_2) - T_3(\log s,\ \log s_1,\ \log s_3, m_3, m_2, k_3), \tag{14a}$$

$$T_i(x, x_1, x_i, m_i, m_{i-1}, k_i) = \frac{1}{2}(m_i - m_{i-1})\left\langle (x - x_1) + \frac{1}{k_i}\ln\left\{\frac{\cosh[k_i(x - x_i)]}{\cosh[k_i(x_i - x_1)]}\right\}\right\rangle, \tag{14b}$$

where m_i is the slope of the linear segment i, s_i is the matric suction at the intersection between segment i and segment $i - 1$, k_i is the curvature parameter between segment i and segment $i - 1$, m_1 is the slope of the initial drying line, s_1 is the matric suction at w_s, and n is the number of linear segments where for unimodal SWCC, $n = 3$. Hence, by changing w_s in Eq. (14a) into $w_{s,f}$ and s_2 into $s_{2,f}$, correction for the density can be done. The value of $s_{2,f}$ can be obtained as follows [24]:

$$s_{2,f} = s_{2,0}10^{(w_{s,0} - w_{s,f})/(m_2 - m_1)}. \tag{15}$$

Conversion between SWCC-w and volumetric-based SWCC (SWCC-θ) and degree of saturation-based SWCC (SWCC-S) can be done by using the shrinkage curve [12,28] by using Eqs. (1) and (2). Leong and Wijaya [29] proposed a shrinkage curve equation for normal shrinkage as follows:

$$e(w) = e_{\min} + \frac{G_s}{2S}\left(w + \frac{1}{c}\ln\left[\frac{\cosh(c(w - \mathrm{SL}))}{\cosh(c \cdot \mathrm{SL})}\right]\right), \quad (16)$$

where $e_{\min}$ is the minimum void ratio, SL is the shrinkage limit, and c is the shrinkage curve empirical parameter, which can be obtained as follows [59]:

$$c = \frac{4.32G_s}{S_0 e_{\min}}. \quad (17)$$

SL was estimated by using LL and PL based on the Casagrande method [60,61] where SL can be determined as follows:

$$\mathrm{SL} = 46.355\left(\frac{\mathrm{LL} + 43.5}{\mathrm{PI} + 46.355}\right) - 43.5. \quad (18)$$

The minimum void ratio ($e_{\min}$) can be estimated through the following relationship [18,28]:

$$\frac{e_{\min}}{\mathrm{SL}} = \frac{G_s}{S_0}. \quad (19)$$

Table 2: VG curve-fitting parameters

Curve-fitting parameters	Values
a_v	7.2×10^{-7}
n_v	0.670
m_v	37.712
w_r (%)	0.096
w_s (%)	32.332

Table 3: Physically significant parameters

Reconstituted soil			
w	32.33	%	
w = 32.33%	**m_i**	**s_i (kPa)**	**k_i**
1	0.18	0.1	
2	18.01	570.0	1.15
3	0.0003	32500.0	3.20
***In situ* density**			
w	39.53	%	
w = 35.67%	**m_i**	**s_i (kPa)**	**k_i**
1	0.18	0.1	
2	18.01	224.9	1.15
3	0.0003	32500.0	3.20

4 Test results and discussion

Figure 12 shows the SWCC of the Cimanggung soil fitted with the VG [10] SWCC equation with the curve-fitting parameters for the VG [10] SWCC equation shown in Table 2. It can be seen that the UGT polymer tensiometer measurement results show good fitting with the VG equation. In order to correct the density of the reconstituted soil into the *in situ* density, parameters for Wijaya and Leong [58] must first be determined to fit the SWCC determined from the VG [10] SWCC equation and then corrected for the *in situ* density according to the procedure described in the study of Wijaya and Leong [24]. Parameters for the Wijaya and Leong [58] SWCC equation are shown in Table 3, while the corrected curve is shown in Figure 12.

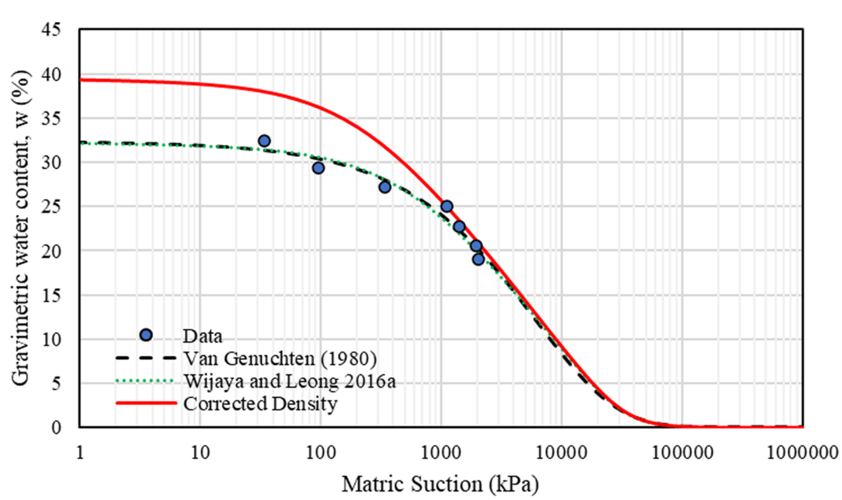

Figure 12: SWCC based on FRT.

Table 4: Parameters of the shrinkage curve

Required parameters	Values
G_s	2.53
S_0 (%)	100
SL	22
e_{min}	0.548
C	9

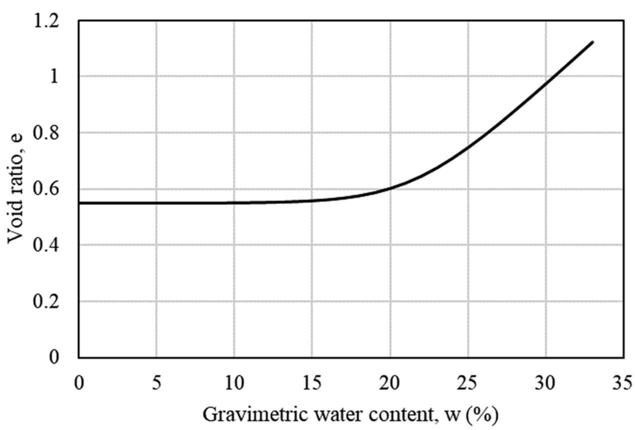

Figure 13: Obtained shrinkage curve.

According to Eq. (18), SL is 22, and e_{min} determined from Eq. (19) is 0.548, as shown in Table 4. Hence, by using Eq. (16), the shrinkage curve can be obtained and is shown in Figure 13. The shrinkage curve can then be used to convert SWCC-*w*, which has been corrected for *in situ* density, into SWCC-θ and SWCC-*S*.

Figure 14 shows the SWCC-θ obtained from the measurement (corrected with *in situ* density) and also SWCC-θ

Table 5: Chin's 1-point method empirical parameters

Empirical parameters	Values (fit 341 kPa)	Values (fit 1,111 kPa)
χ	67.457	98.183
a_f	560.104	486.361
n_f	0.377	0.438
m_f	0.286	0.372
h_r	798.645	751.044
θ_s	0.501	0.501

estimated based on Chin's 1-point method. The sensitivity study on Chin's 1-point method was carried out by using two data points. The first data point was observed at the soil suction of 341 kPa, and the second data point was at the soil suction of 1,111 kPa. Parameters for the Chin's 1-point method are shown in Table 5. It is important to note that the range of measurements is only up to 2,000 kPa, and it shows that the measured SWCC-θ and SWCC-θ estimated from Chin's 1-point method (predicted by using 341 kPa suction and 1,111 kPa suction) agree very well in this measurement range. The difference in SWCC beyond the range of measurements could be due to the lack of data points which affects the shape of SWCC.

Figure 15 shows the measured SWCC-*S* along with estimated SWCC from the study of Perera *et al.* [55] and from Chin's 1-point method. SWCC-θ from Chin's 1-point method is converted into SWCC-*S* by using the shrinkage curve. It is shown that Chin's 1-point method for fit at 341 and 1,111 kPa have roughly the same AEV. However, Perera *et al.*'s [55] SWCC-*S* equation underestimated the AEV, and the curve deviated significantly with the measured SWCC. It is understandable that Chin's 1-point method gives higher accuracy

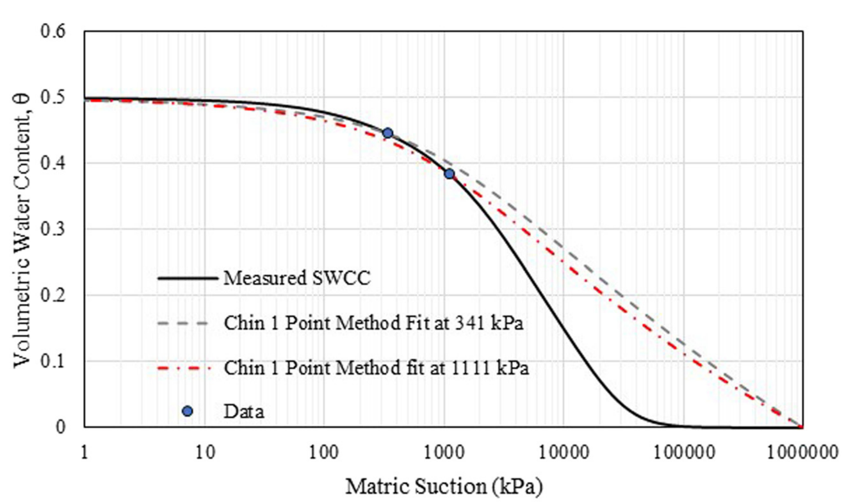

Figure 14: SWCC-θ obtained from our measurement and the Chin-1 point method.

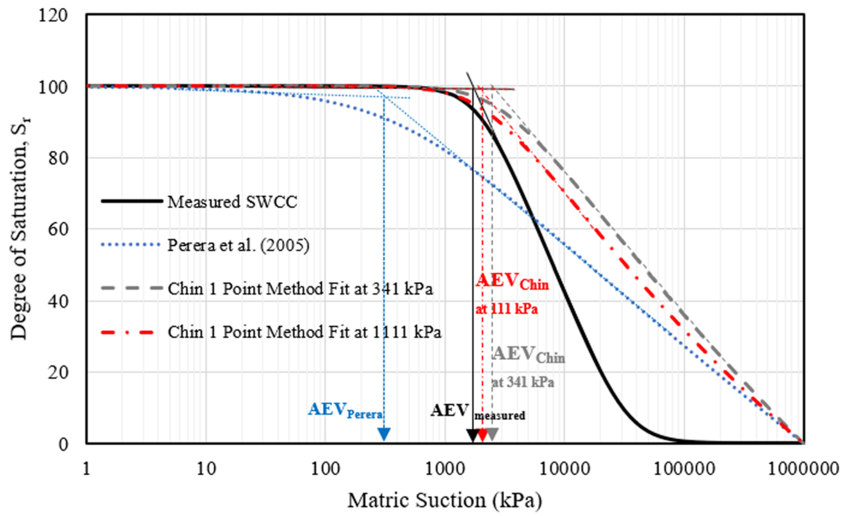

Figure 15: SWCC-*S* obtained from our measurement and the Perera *et al.* [55] method.

as it is based on 1 data point. However, considering that obtaining 1 data point is not difficult, it is recommended to use Chin's 1-point method to estimate both SWCC-θ and SWCC-*S*. Chin's 1-point method can also be applied by inserting the polymer tensiometer *in situ* and directly taking the *in situ* soil for water content measurement. Such procedures allow for rapid and reliable SWCC estimation. The SWCCs can then be used as input parameters along with an unsaturated permeability function to assess the effect of rainfall infiltration on Cimanggung slope failure.

It could be concluded that Chin's 1-point method yields a close estimation within the suction range. Meanwhile, the Perera *et al.* method underestimates the AEV and the predicted curve deviates significantly from the measured SWCC. Hence, Chin's 1-point method is recommended for predicting SWCCs in Cimanggung Village and used as the volcanic soil SWCC database.

5 Conclusions

Determination of SWCC on slope failure is difficult due to the uncertainty in determining the density of the debris as the soil has been altered from its original condition (before slope failure). In this article, a new method and procedure to generate SWCC-*w*, SWCC-θ, and SWCC-*S* for soil located at slope failure by using the full range of suction has been developed. The key findings are as follows:

- In this procedure, it is recommended to obtain the soil sample from the debris, reconstitute the soil sample, and then obtain the SWCC-*w*.
- The validation of the new procedure has been done to obtain the SWCC of reconstituted soil located at the Cimanggung village. SWCC-*w*, SWCC-θ, and SWCC-*S* corrected for *in situ* density have been obtained.
- The measured SWCC is also compared with those of Chin's 1-point method [57] and Perera *et al.*'s [55] method.

Acknowledgement: The authors would like to thank Parahyangan Catholic University for the support, P.T. Geotechnical Engineering Consultant for providing the data, documentation, and visual inspection at the site, and Wykeham Farrance LTD for providing the full-range tensiometer.

Funding information: The authors state no funding was involved.

Author contributions: All authors have accepted responsibility for the entire content of this manuscript and approved its submission.

Conflict of interest: The authors declare no conflict of interest.

References

[1] Fredlund DG, Rahardjo H, Fredlund MD. Unsaturated soil mechanics in Engineering practice. Hoboken, New Jersey: John Wiley & Sons, Inc; 2012.

[2] Bao C, Gong B, Zhan L, editors. Keynote Lecturer, Properties of unsaturated soils and slope stability of expansive soils.

Proceedings of the 2nd International Conference on Unsaturated Soils (UNSAT 98). Beijing, China: International Academic; 1998.
[3] Goh SG, Rahardjo H, Leong EC. Shear strength equations for unsaturated soil under drying and wetting. ASCE J Geotech Geoenviron Eng. 2010;136(4):594–606.
[4] Khalili N, Khabbaz MH. A unique relationship for c for the determination of the shear strength of unsaturated soils. Géotechnique. 1998;48(5):681–7.
[5] Lee IM, Sung SG, Cho GC. Effect of stress state on the unsaturated shear strength of a weathered granite. Can Geotech J. 2005;42(2):624–31.
[6] Rassam DW, Cook FJ. Predicting the shear strength envelope of unsaturated soils. Geotech Test J. 2002;25(2):215–20.
[7] Rassam D, Williams D. Unsaturated hydraulic conductivity of mine tailings under wetting and drying conditions. Geotech Test J. 1999;22(2):144–52.
[8] Tekinsoy MA, Kayadelan C, Keskin MS, Soylemaz M. An equation for predicting shear strength envelope with respect to matric suction. Comput Geotech. 2004;31(7):589–93.
[9] Hunt AG. Comparing van Genuchten and Percolation theoretical formulations of the hydraulic properties of unsaturated media. Vadose Zone J. 2004;3(4):1483–8.
[10] van Genuchten MT. A closed-form equation for predicting the hydraulic conductivity of unsaturated soils. Soil Sci Soc Am J. 1980;44(5):892–8.
[11] Wijaya M, Leong EC. Discussion of "Permeability function for oil sands tailings undergoing volume change during drying". Can Geotech J. 2019;56(2):300–2.
[12] Zhang F, Wilson GW, Fredlund DG. Permeability function for oil sands tailings undergoing volume change during drying. Can Geotech J. 2017;55(2):191–207.
[13] Fredlund DG, Xing A, Huang S. Predicting the permeability function for unsaturated soils using the soil-water characteristic curve. Can Geotech J. 1994;31(4):533–46.
[14] Zhai Q, Rahardjo H, Satyanaga A, Dai G. Estimation of the soil-water characteristic curve from the grain size distribution of coarse-grained soils. Eng Geol. 2020;267:105502.
[15] Zhai Q, Rahardjo H, Satyanaga A, Zhu Y, Dai G, Zhao X. Estimation of wetting hydraulic conductivity function for unsaturated sandy soil. Eng Geol. 2021;285:106034.
[16] Zhai Q, Rahardjo H, Satyanaga A, Dai G, Du Y. Estimation of the wetting scanning curves for sandy soils. Eng Geol. 2020;272:105635.
[17] Ni J, Gu J, Zhao X. A hypoplastic model for unsaturated sand accounting for drying and wetting cycles. Comput Geotech. 2024;165:105879.
[18] Wijaya M, Leong EC, Rahardjo H. Effect of shrinkage on air-entry value of soils. Soils Found. 2015;55(1):166–80.
[19] Zhai Q, Zhu Y, Rahardjo H, Satyanaga A, Dai G, Gong W, et al. Prediction of the soil–water characteristic curves for the fine-grained soils with different initial void ratios. Acta Geotech. 2023;18(10):5359–68.
[20] Zhai Q, Rahardjo H, Satyanaga A, Dai G-L, Du Y-J. Effect of the uncertainty in soil-water characteristic curve on the estimated shear strength of unsaturated soil. J Zhejiang Univ-Sci A. 2020;21(4):317–30.
[21] Qian Z, Harianto R, Alfrendo S. Uncertainty in the estimation of hysteresis of soil–water characteristic curve. Environ Geotech. 2019;6(4):204–13.
[22] Salager S, El Youssoufi MS, Saix C. Definition and experimental determination of a soil-water retention surface. Can Geotech J. 2010;47(6):609–22.
[23] Jotisankasa A, Ridley A, Coop M. Collapse behavior of compacted silty clay in suction-monitored oedometer apparatus. J Geotech Geoenviron Eng. 2007;133(7):867–77.
[24] Wijaya M, Leong EC. Modelling the effect of density on the unimodal soil-water characteristic curve. Géotechnique. 2017;67(7):637–45.
[25] Salager S, Ferrari A, Nuth M, Laloui L. Investigations on water retention behaviour of deformable soils. Unsaturated Soils-Alonso & Gens (eds). Barcelona, Spain: Taylor & Francis Group; 2011. p. 485–90.
[26] Yao Y, Ni J, Li J. Stress-dependent water retention of granite residual soil and its implications for ground settlement. Comput Geotech. 2021;129:103835.
[27] Bordoloi S, Ni J, Ng CWW. Soil desiccation cracking and its characterization in vegetated soil: A perspective review. Sci Total Environ. 2020;729:138760.
[28] Fredlund MD, Wilson GW, Fredlund DG. Representation and estimation of the shrinkage curve. In: Jucá JFT, de Campos TMP, Marinho FAM, editors. 3rd International Conference on Unsaturated Soils (UNSAT 2002). Recife, Brazil; 2002. p. 145–9.
[29] Leong EC, Wijaya M. Universal soil shrinkage curve equation. Geoderma. 2015;237–238:78–87.
[30] UInspire. Situation Report #8 Rrespon Bencana Longsor Kampung Daud/Bojong Kondang, Desa Cihanjuang, Kec. Cimanggung, Kab. Sumedang, Prov. Jawa Barat. Indonesia; 2020.
[31] Adiguna GA, Wijaya M, Rahardjo PP, Sugianto A, Satyanaga A, Hamdany AH. Practical approach for assessing wetting-induced slope failure. Appl Sci. 2023;13(3):1811.
[32] Ridley AM, Burland JB. A new instrument for the measurement of soil moisture suction. Géotechnique. 1993;43(2):321–4.
[33] Guan Y, Fredlund DG. Use of the tensile strength of water for the direct measurement of high soil suction. Can Geotech J. 1997;34(4):604–14.
[34] Leong EC, Lee CC, Low KS. An active control system for matric suction measurement. Soils Found. 2009;49(5):807–11.
[35] Stannard DI. Tensiometer-theory, construction and use. ASTM Int. 1992;15(1):35–51.
[36] Hilf JW. An investigation of pore-water pressure in compacted cohesive soils. Denver, CO: Tech. Memo. No. 654, U. S. Dep. of the Interior, Bureau of Reclamation, Design and Construction Div.; 1956.
[37] Wijaya M, Leong EC. Performance of high-capacity tensiometer in constant water content oedometer test. Int J Geo-Eng. 2016;7(1):13.
[38] Wijaya M. Compression, shrinkage and wetting-induced volume change of unsaturated soils. Ph.D. thesis. Singapore: Nanyang Technological University; 2017.
[39] Lourenço SDN, Gallipoli D, Toll DG, Evans FD. On the measurement of water pressure in soils with high suction tensiometers. Geotech Test J. 2009;32(6):565–71.
[40] Chen R, Liu J, Li JH, Ng CWW. An integrated high-capacity tensiometer for measuring water retention curves continuously. Soil Sci Soc Am J. 2015;79(3):943–7.
[41] He L, Leong EC, Elgamal A, editors. A miniature tensiometer for measurement of high matric suction. Unsaturated soils 2006. Reston Va [Great Britain]: American Society of Civil Engineers; 2006.

[42] Oliveira OM, Marinho FAM. Suction equilibration time for a high capacity tensiometer. Geotech Test J. 2008;31(1):101–5.
[43] Leong E, He L, Rahardjo H. Factors affecting the filter paper method for total and matric suction measurements. Geotech Test J. 2002;25(3):322–33.
[44] Leong EC, Wijaya M, Tong WY, Lu Y. Examining the contact filter paper method in the low suction range. Geotech Test J. 2020;43(6):1567–73.
[45] Leong E-C, Tripathy S, Rahardjo H. Total suction measurement of unsaturated soils with a device using the chilled-mirror dew-point technique. Géotechnique [Internet]. 2003;53:173–82, http://www.icevirtuallibrary.com/content/article/10.1680/geot.2003.53.2.173.
[46] Bulut R, Leong EC. Indirect measurement of suction. Geotech Geol Eng. 2008;26(6):633.
[47] Hamdany AH, Shen Y, Satyanaga A, Rahardjo H, Lee T-TD, Nong X. Field instrumentation for real-time measurement of soil-water characteristic curve. Int Soil Water Conserv Res. 2022;10(4):586–96.
[48] Degré A, van der Ploeg MJ, Caldwell T, Gooren HPA. Comparison of soil water potential sensors: A drying experiment. Vadose Zone J. 2017;16(4):vzj2016.08.0067.
[49] Durigon A, Gooren HPA, van Lier QdJ, Metselaar K. Measuring hydraulic conductivity to wilting point using polymer tensiometers in an evaporation experiment. Vadose Zone J. 2011;10(2):741–6.
[50] van der Ploeg MJ. Polymer tensiometers to characterize unsaturated zone processes in dry soils. Netherlands: Wageningen Universiteit; 2008.
[51] Peck AJ, Rabbidge RM. Soil-water potential: Direct measurement by a new technique. Science. 1966;151(3716):1385–6.
[52] Peck AJ, Rabbidge RM. Design and performance of an osmotic tensiometer for measuring capillary potential. Soil Sci Soc Am J. 1969;33(2):196–202.
[53] van der Ploeg MJ, Gooren HPA, Bakker G, Hoogendam CW, Huiskes C, Koopal LK, et al. Polymer tensiometers with ceramic cones: direct observations of matric pressures in drying soils. Hydrol Earth Syst Sci. 2010;14(10):1787–99.
[54] Bocking K, Fredlund D. Use of the osmotic tensiometer to measure negative pore water pressure. Geotech Test J. 1979;2:3–10.
[55] Perera YY, Zapata CE, Houston WN, Houston SL. Prediction of the soil-water characteristic curve based on grain-size-distribution and index properties. Adv Pavement Eng. 2005;1–12.
[56] Fredlund DG, Xing A. Equations for the soil-water characteristic curve. Can Geotech J. 1994;31(4):521–32.
[57] Chin KB, Leong EC, Rahardjo H. A simplified method to estimate the soil-water characteristic curve. Can Geotech J. 2010;47(12):1382–400.
[58] Wijaya M, Leong EC. Equation for unimodal and bimodal soil–water characteristic curves. Soils Found. 2016;56(2):291–300.
[59] Wijaya M, Leong EC. Estimation of soil shrinkage curve. Unsaturated soils: Research & Applications. China GuiLin: CRC Press/Balkema; 2015. p. 785–9.
[60] Holtz RD, Kovacs WD, Sheahan TC. An introduction to geotechnical engineering. 2nd edn. United States: Pearson Education, Inc; 2011.
[61] Budhu M. Hoboken NJ, editors. Soil mechanics and foundations. 3rd edn. United States: Wiley; 2010.